Stent deployment in aneurysmatic cerebral vessels: Assessment and quantification of the differences between Fast Virtual Stenting and Finite Element Analysis

Eleonora Flore, Ignacio Larrabide, Lorenza Petrini, Giancarlo Pennati, Alejandro Frangi

HAL is a multi-disciplinary open access archive for the deposit and dissemination of scientific research documents, whether they are published or not. The documents may come from teaching and research institutions in France or abroad, or from public or private research centers.

L'archive ouverte pluridisciplinaire **HAL**, est destinée au dépôt et à la diffusion de documents scientifiques de niveau recherche, publiés ou non, émanant des établissements d'enseignement et de recherche français ou étrangers, des laboratoires publics ou privés.

Stent deployment in aneurysmatic cerebral vessels: Assessment and quantification of the differences between Fast Virtual Stenting and Finite Element Analysis

Eleonora Flore[1,2], Ignacio Larrabide[2,1], Lorenza Petrini[4], Giancarlo Pennati[4], Alejandro Frangi[1,2,3]

Center for Computational Imaging and Simulation Technologies in Biomedicine (CISTIB) -
[1] Universitat Pompeu Fabra (UPF); [2]Networking Center on Biomedical Research (CIBER-BBN); [3]Institució Catalana de Recerca i Estudis Avançats (ICREA), Barcelona Spain;
[4] Laboratory of Biological Structure Mechanics, Politecnico di Milano, Milano, Italy.

Abstract. To assess the efficacy of stenting procedure in the treatment of cerebral aneurysms, a tool predicting accurately and with fast execution time the stent released configuration could be very useful. The aim of this work is to propose a first validation of the Fast Virtual Stenting method by comparing its results with the ones achieved with Finite Element Analysis. A series of parametric models has been set varying the geometries of the stent, the vessel and the aneurysmal neck, and the differences between the two methods have been evaluated comparing the released configurations in corresponding models. Results show a quite fine match between the two methodologies, accompanied by a significant reduction in the computational costs gained with FVS. In this way, this method seems to be a promising tool to help clinicians choosing the best treatment option.

Keywords: Stent, cerebral aneurysm, Fast Virtual Stenting method, Finite Element Analysis.

1 Introduction

Intracranial stenting procedure seems to be a valid treatment option for cerebral aneurysms which are not suitable for conventional therapies. Among others, Barath et al. [1] illustrated that the presence of a low porous stent in an anatomically shaped aneurysm model damps the flow inside the pouch and reduces the wall shear stresses. These effects create a stagnant region inside the aneurysm and could decrease its risk of rupture. Moreover, Lieber et al. [2] have shown that the impedance exerts by the stent to the flow into the aneurysmal sac could be maximized by controlling the stent design. Besides all of the design features, Hirabayashi et al. [3] illustrated that the position and the released configuration of the stent play a significant role in modifying the blood flow and must be taken into account. Therefore, a methodology predicting the disposition of stents when released within patient-specific vessel geometries is necessary to evaluate the efficacy of such devices and would be useful to clinicians in selecting the most appropriate treatment option for each pathological case.

In this light, computational simulations of the stent release could be powerful tools during treatment planning to assess the efficacy of stenting procedure. To be really effective for clinical applications, they have to provide reliable information with a computational time in the order of minutes.

Finite Element Analysis (FEA) has been extensively used to study both the mechanical behavior of stents during their deployment and the interaction between released stents and the vessel wall. In particular, the influence of stent material and geometry on its expansion and on the tissue response has been widely investigated [4-5]. As the presence of curvatures in the vessels and their specific anatomy affect the stent conformability, Wu et al. [6] and Gijsen et al. [7] performed stent deployment simulations in curved vessels and in one patient derived model respectively. However, because of the complexity of these models, including high constitutive and kinematic non linearities, and due to the required high computational costs, so far FEA simulations are not feasible for a broad use with patient specific geometries.

A different method allowing the prediction of the stent released shape is based on deformable models. The first techniques were proposed by Appanaboyna et al. [8] and Valencia et al. [9] and were able to release a stent inside a patient specific vessel. However, they didn't consider physical and geometrical characteristics of the stents which can guarantee realistic stent configurations. Instead, the Fast Virtual Stenting (FVS) methodology, proposed by Larrabide et al. [10], takes into account the geometric properties of the stents and was successfully applied with low computational costs to virtual stent deployment in real vessel geometries.

Nevertheless, the lack of an exhaustive validation of this method requires further assessments of its results. The aim of this work is therefore to evaluate and quantify the differences in simulating the stent released configuration between FVS method and FEA.

2 Methods

A series of parametric models has been set to simulate the release of two selfexpanding stents inside cerebral vessels hosting aneurysms. With reference to the design of the Neuroform stent (Boston Scientific, Natick, MA, USA), two stents with different nominal diameters (3 and 4.5 mm) were considered. According to the information provided by the manufacturer, these stents are supposed to be implanted in cerebral vessels with a mean diameter within 2.1-2.5 mm and 3.6-4 mm respectively. Two idealized straight vessel geometries were then used for each stent, taking into account the diameter values mentioned above. As the aneurysm dome is not supposed to affect the stent released configuration, only the aneurysm orifice was reproduced. Three different necks were considered for each vessel geometry: two of them have a circular shape with a main dimension proportional to the vessel diameter, whereas the third one has an elliptic shape, whose major axis is equal to the stent diameter and the minor axis is proportional to the vessel diameter.
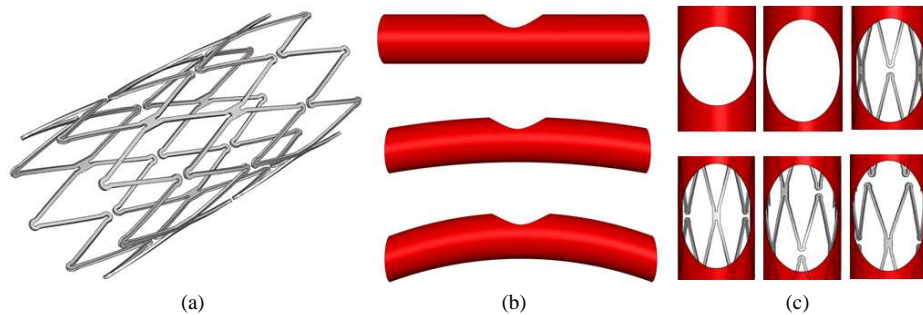
<table>
<tr><td>(a)</td><td>(b)</td><td>(c)</td></tr>
</table>

Fig. 1. Stent (a) and vessel (b) geometries; in (c) are shown the two neck shapes and the reference stent position on the top, while down the different orientations of the stent with respect to its axis are depicted: starting from the left, these models are named S2-C2-P1, S2-C2-P2, S2-C2-P3.

Table 1. Table summarizing the geometric parameters of the stents and the vessels considered in the different experiments of the study. All the dimensions are expressed in mm.

Model	Stent Diameter	Vessel Diameter	Curvature Radius	Neck shape	Neck dimension
S1-V1-N1	3	2.1	∞	circular	d = 2.25
S1-V1-N2	3	2.1	∞	circular	d = 1.5
S1-V1-N3	3	2.1	∞	elliptic	2a = 3 ; 2b = 2.25
S1-V2-N1	3	2.5	∞	circular	d = 1.89
S1-V2-N2	3	2.5	∞	circular	d = 1.26
S1-V2-N3	3	2.5	∞	elliptic	2a = 3 ; 2b = 1.89
S2-V3-N1	4.5	3.6	∞	circular	d = 3.6
S2-V3-N2	4.5	3.6	∞	circular	d = 2.4
S2-V3-N3	4.5	3.6	∞	elliptic	2a = 4.5 ; 2b = 3.6
S2-V4-N1	4.5	4	∞	circular	d = 3.24
S2-V4-N2	4.5	4	∞	circular	d = 2.16
S2-V4-N3	4.5	4	∞	elliptic	2a = 4.5 ; 2b = 3.24
S2-C1-N3	4.5	3.6	20	elliptic	2a = 4.5 ; 2b = 3.24
S2-C2-N3 *	4.5	3.6	10	elliptic	2a = 4.5 ; 2b = 3.24

d denotes the diameter of the circular necks, 2a and 2b are respectively the major axis and the minor axis of the elliptic necks; *the stent, vessel and neck characteristics of this model have been used in the simulations executed with different stent orientations illustrated in Figure 1 (d).

Since the conformability of intracranial stents is highly influenced by the curvature of cerebral vessels and their axial orientation, two curved vessels geometries with elliptic aneurysm necks and three different rotations of the stent with respect to its axis have been also taken into account. In particular, we considered different position of the stent in the vessel with the greatest curvature, which is expected to modify more the stent configuration. Details of the models are depicted in Figure 1 and the geometric features of the stents and the vessels considered in the study are resumed in Table 1. More details on the models definition and the simulations executed both with FVS method and FEA are provided in the following sections.

2.1 Fast Virtual Stenting method

The methodology proposed by Larrabide et al. [14] is based on constrained deformable simplex meshes. This approach consists mainly in defining a second order differential equation to deform a simplex mesh under the effect of particular constrains (internal and external forces). The authors extended the method adopted by Montangnat and Delingette [15], by introducing a new force that encodes geometric constrains concerning the specific stent design. In [15] more definitions and additional information on simplex meshes can be found.

According to the geometric characteristics of the stents S_1 and S_2 (strut layout, strut length, angle between the struts, etc.), the stent meshes have been created by defining, over a subset of points constituting the simplex mesh, the sets of nodes corresponding to the extremities of the stent struts and their connectivity. To take into account the specific geometry of each stent, further parameters have to be specified: stent crimped and nominal diameters and the strut width.

In order to position the stent in the appropriate vessel segment, generating its initial conditions, the vessel centerline has been extracted and one of its points selected to be the starting point for the simplex mesh. The second order differential equation chosen to expand the simplex mesh in the vessel has been conveniently discretized by finite differences, obtaining:

$$p_i^{n+1} = p_i^n + (1-\gamma)(p_i^n - p_i^{n-1}) + \alpha(f_{smooth}(p_i^n) + \chi f_{length}(p_b^n)) + (1-\alpha) f_{ext}(p_i^n). \qquad (1)$$

where p_i is a point of the simplex mesh and n is the iteration number. The terms f_{smooth} and f_{length} represent the internal and the stent-shape constraining force; in particular, the last one has been introduced to preserve the strut length during the expansion. f_{ext} corresponds to an attractive force moving the stent mesh from the initial condition towards the vessel wall; this force is stopped when a mesh point is closer than a given value ε to the vessel wall, set equal to half the strut radial thickness. The constants α and χ are weighting parameters for the different forces. The values to be assigned to the parameters α and χ have been chosen according to previous work [10]. FVS simulations have been carried out on an Intel ® CoreTM Duo CPU T7300 2.00 GHz with 2 Gb of memory.

2.2 Finite Element Analysis

FEA simulations have been performed by means of the commercial code ABAQUS/Standard (Simulia Corp, Providence, RI, USA) and executed on a Cluster with a parallelization of 4 CPUs, each one with 4Gb of memory.

Vessels

The idealized vessels have been modeled as rigid bodies and have been discretized with meshes of 4-node shell elements, which numbers vary within 52880 and 66450, according to the particular geometry. Simplifying the vessel wall as rigid clearly involves a reduction in the complexity of the models, and does not allow considering the real interplay between the vessel and the stent. However selfexpanding stents are supposed to exert a lower radial force to the vessel with respect to balloon-expandable

ones [4]. Moreover, Tanaka et al. [12] showed that the release of open-cell nitinol stents in a silicon model of the human carotid artery preserves the geometry of the carotid bifurcation and the ICA curve and doesn't induce a straightening of the vessel segment with the stent. For these reasons, we assume potential expansions or morphological modifications of the vessels induced by the stent negligible in this first validation.

Stents

The geometries of the two stents have been created using the commercial CAD software Rhinoceros 4.0 Evaluation (McNeel & Associates, Indianapolis, IN, USA), following the information both obtained from a μ-CT scan of the stents and provided by the manufacturer. The stents have been meshed with 8-node brick elements; the number of elements is 110550 for the stent S_1 and 158740 for the stent S_2. The mechanical behavior of the Ni-Ti alloy which self-expanding stents are made of has been described by the use of a previously developed user subroutine [13]. The typical mechanical characteristics of the Neuroform stent are not available; hence average values derived from literature were chosen as algorithm input parameters (see Table 2) [4,5,13]. In Figure 2 the typical pseudo-elastic uniaxial stress-strain (a) and threshold transformation stress-temperature (b) curves are illustrated and the main input parameters indicated.

Table 2. Input parameters required by the user subroutine describing Ni-Ti alloy behavior.

|			
E	*elastic modulus, assumed equal for the martensite and the austenite*	**70000**	[MPa]
ν	*Poisson's coefficient*	**0.3**	[-]
ε_L	*transformation strain*	**0.06**	[-]
H	*transformation phase tangent modulus*	**3500**	[MPa]
β	*coefficient of the stress component inducing transformation-temperature relation, according to $\sigma_s=\sigma_0+R$ and $\sigma_0=\beta<T-M_f>$; σ_0 is the stress value indicating the mean value of the mechanical hysteresis and σ_s is the stress threshold value at which the austenite to martensite transformation starts*	**5**	[MPa/K]
M_f	*martensite finish transformation temperature*	**273.6**	[K]
T	*current temperature (SMA in austenitic phase)*	**310.15**	[K]
R	*half of the mechanical hysteresis amplitude in the uniaxial tension-compression case*	**50**	[MPa]
m	*coefficient related to the asymmetric behavior of SMA in tension and compression*	**1**	[-]
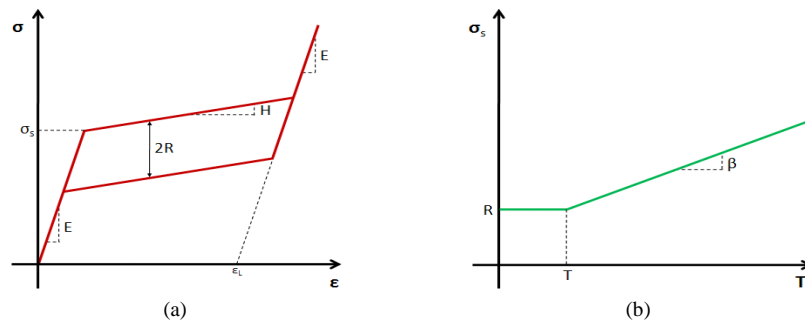
Fig. 2. Uniaxial pseudo-elastic stress-strain curve (a) and threshold transformation stress-temperature curve (b) for a Ni-Ti alloy. The main input parameters required by the user subroutine are indicated.

Boundary conditions and steps of the analysis

To simulate the stent release two steps have been defined in the analysis: (i) the crimping of the stent and (ii) the selfexpansion of the stent until it contacts the vessel wall. Crimping procedure consists in a radial compression of the stent and its insertion into a low profile delivery system, as intracranial self expandable stents are characterized by an initial diameter bigger than the one of the vessel in which are supposed to be implanted. This procedure has been simulated by uniformly applying a negative radial displacement to the nodes of the internal surface of the stent. In order to prevent vessels and stents rigid motions, appropriate sets of nodes in the stent and the vessel were constrained in the axial and tangential directions.

After this first step, every displacement in radial direction has been removed in order to allow the free expansion of the stent, thanks to the pseudoelasticity property of its material, and its adjustment to the vessel geometry. The contact between the stent outer and the vessel inner surfaces has been modeled with a frictionless hard contact interaction.

3 Results

To assess the differences between both methods, the stent released configurations have been compared for each scenario. In order to quantify these differences, the distance between corresponding nodes in the two models has been computed. The error has been then calculated by comparing these distances to the vessel diameters. Particular attention has been paid to the error detected on the nodes located in the aneurysm orifice. Indeed, this is the region in which the effect of the stent on the blood flow is more significant for aneurysm treatment; for this reason, predicting the most realistic stent released configuration in this area is extremely important. Figure 3 (a) depicts the box plot for the errors in all the models, and also shows error average values.
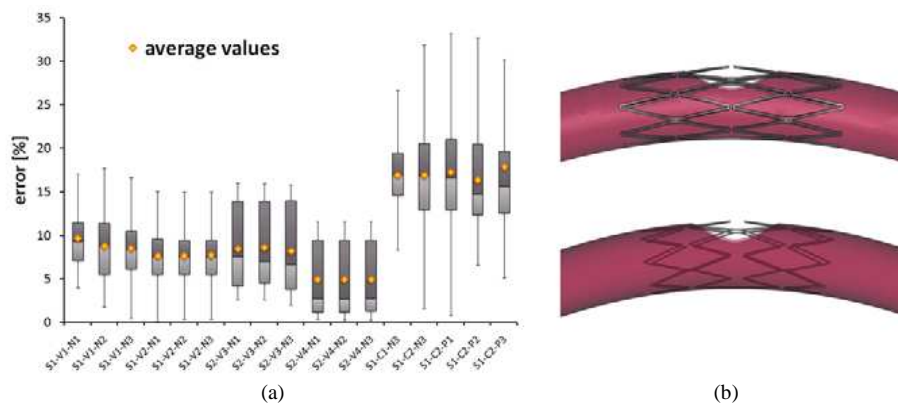
Fig. 3. Box plot for the error between corresponding nodes in FEA and FVS models (a); the stent final configurations in the model S2-V4-N3 are depicted in (b): on the top is shown the FEA model and down is the FVS model.

It can be noticed that while the mean values observed releasing the stents into straight vessels are within 5% and 10%, in the models with curved vessels mean errors greater than 15% have been achieved. The final FEA and FVS configurations of the stent in one of the curved vessel geometries are shown in Figure 3 (b). It has to be remarked that, as we expected, the curvature of the vessel induced a more pronounced protrusion of the struts in the neck. With the aim of investigating more deeply how these errors reflect the differences in the stent release configurations, the errors in radial, circumferential and longitudinal directions have been evaluated for the models with straight vessels. The comparison between the maximum radial and longitudinal error is presented in Figure 4 (a). It can be observed that the maximum radial error, which can be considered a first parameter to evaluate the differences in the stent expansion and correspond for all the models to nodes located in the neck, is significantly lower than the longitudinal one for all the models. As for the models with curved vessels, the maximum error is not observed in correspondence to the aneurysm neck; however the values detected in this region reveal a quite meaningful difference between FEA and FVS methods, especially for the models S1-C2-N3 and S1-C2-P1.

Moreover, the most significant difference between the two methods consists in the computational time and, as previously mentioned, resources required. Indeed, while FEA simulations run in almost two hours each, the average time required for the stent release with FVS method was 5.2727 s with a standard deviation of 0.64667 s, with an exceptional gain of computational time.
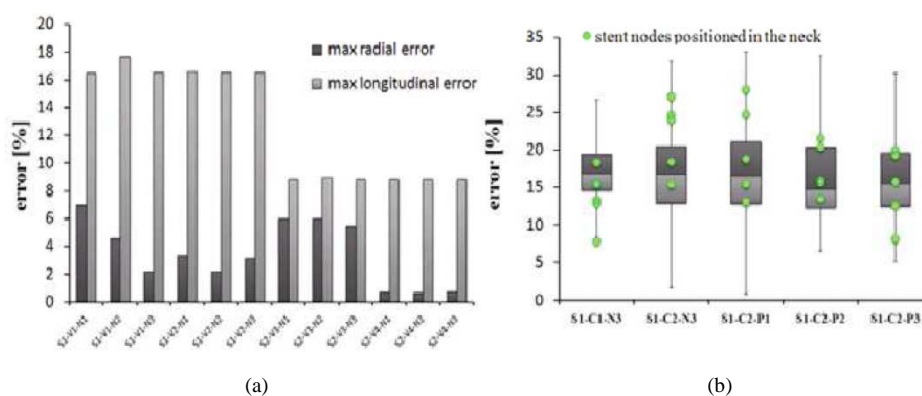
(a)   (b)

Fig. 4. Maximum radial and longitudinal errors obtained releasing the stents in straight vessel geometries (a); the error computed for the nodes of the stent positioned in the aneurysm neck is superimposed to the box plots for the error obtained with the curved vessel geometries (b).

4 Conclusion and Future Works

Fast Virtual Stenting method could be a valid tool to help clinicians evaluating the efficacy of stenting procedure in the treatment of cerebral aneurysms. Indeed, our results, obtained with idealized vessel geometries, indicate that it could provide results close to the ones obtained with FEA simulations in the same conditions, with a significant reduction of the computational time. The possibility to simulate the stenting procedure with fast execution times is definitely fundamental for clinical applications, in particular during treatment planning.

However, in this study, the correspondence between FVS and FEA stent deployment is limited for straight and less curved vessels, while cerebral vasculature could be characterized by more accentuate curvatures. Further work is then required to validate FVS method with more physiological curvature values and patient specific vessel geometries. Additional optimizations of the algorithm parameters for different stent designs and an evaluation of the effects induced by a more realistic description of the vessel material are also necessary to assess the quality of this methodology and are currently work in progress. In the end, it should be verified whether and how the differences in the released configuration obtained with FEA and FVS really induce significant change in the vessel and aneurysm fluid dynamics.

References

1. Barath, K., Cassot, F., Rüfenacht, D.A., Fasel, J.H.: Anatomically Shaped Internal Carotid Artery Aneurysm In Vitro Model for Flow Analysis to Evaluate Stent Effect. Am. J. Neuroradiol., 25 (10), 1750--1759 (2004)
2. Lieber, B.B., Livescu, V., Hopkins, L.N., Wakhloo, A.K.: Particle Image Velocimetry Assessment of Stent Design Influence on Intra-Aneurysmal Flow. Annals of Biomedical Engineering, 30, 768--777 (2002)
3. Hirabayashi, M., Ohta, M., Rüfenacht, A., Chopard, B.: A Lattice Boltzmann Study of Blood Flow in Stented Aneurysm. Future Generation Computer System, 20, 925--934 (2004)
4. Migliavacca, F., Petrini, L., Massarotti, P., Schievano, S., Auricchio, F., Dubini G.: Stainless and Shape Memory Alloy Coronary Stents: A Computational Study on The Interaction with the Vascular Wall. Biomech. Model. Mechanobiol., 2, 205--217 (2004)
5. Wu W., Qi M., Liu X.P., Yang D.Z., Wang W.Q.: Delivery and Release of Nitinol Stent in Carotid Artery and their Interactions: a Finite Element Analysis. J. Biomech., 40, 3034--40 (2007)
6. Wu, W., Wang, W.Q., Yang, D.Z., Qi, M.: Stent Expansion in curved Vessel and their Interactions: A Finite Element Analysis. J. Biomech., 40, 2580--2585 (2007)
7. Gijsen, F.J.H., Migliavacca, F., Schievano S., Socci, L., Petrini, L., Thury, A., Wentzel, J.J., van der Steen, A.F.W., Serruys, P.W.S., Dubini, G.: Simulation of Stent Deployment in a Realistic Human Coronary Artery. Biomed. Eng. Online, 6, 7--23 (2008)
8. Appanaboyna, S., Mut, F., Lohner, R., Putman, C.M., Cebral, J.R.: Computational Fluid Dynamics of Stented Intracranial Aneurysms Using Adaptive Embedded Unstructured Grids. Int. J. Numer. Meth. Fluid., 57(5), 475--493 (2008)
9. Valencia, L.F., Montagnat, J., Orkisz, M.: 3D Graphicl Models For Vascular-Stent Pose Simulation. Innovations Technol. Biol. Med. 28(2), 65--71 (2007)
10. Larrabide, I., Radaelli, A., Frangi, A.: Fast virtual stenting with deformable meshes: application to intracranial aneurysms. MICCAI08 - LNCS 5242 - Part II - 790-797, 6th-10th September 2008, New York, NY, USA
11. Tanaka, N., Martin J.B., Tokunaga K., Abe T., Uchiyama, Y., Hayabuchi, N., Berkfeld, J., Rüfenacht, D.A.: Conformity of Carotid Stents with Vascular Anatomy: Evaluation in Carotid Models. Am. J. Neuroradiol., 25, 601--607 (2004)
12. Montagnat, J., Delingette, H.: 4D deformable Models with Temporal Constraints: Application to 4D Cardiac Image Segmentation. Med. Image Anal., 9, 87--100 (2005)
13. Auricchio, F., Petrini, L.: A Three-dimensional Model Describing Stress-Temperature Induced Solid Phase Transformations: Solution Algorithm and Boundary Value Problems. Int. J. Numer. Meth. Eng., 61, 807--836 (2004)